Journal of Materials Science & Surface Engineering Vol. 3 (2), 2015, pp 227-231

Contents lists available at http://www.jmsse.org/

Journal of Materials Science & Surface Engineering

Nanoindentation Based Fatigue Analysis of Semiconductor Bridge (SCB) for Mechanical Reliability

Pradnya M. Bodhankar[1*], Chetan Gurada[2], Shrihari Shinde[1], H. Muthurajan[1],Virendra Kumar[3]

[1]*National Centre for Nanoscience and Nanotechnology, University of Mumbai, India.*
[2]*Department of Physics, University of Mumbai, India.*
[3]*Armament Research and Development Establishment, Pune, India.*

Article history

Received: 01-July-2015
Revised: 11-July-2015
Available online: 26-Aug-2015

Keywords:
Fatigue Analysis,
Electro explosive device (EED),
Semiconductor bridge (SCB),
Hardness

Abstract

In addition to military and aerospace applications, electro explosive devices (EED) are extensively used in civil applications such as air bags in automotive industries, tunnel constructions, demolition of complex structure, commercial rock blasting, mining, seismic exploration, etc. Semiconductor bridge (SCB) igniters are advanced electro explosive devices which are usually fabricated using state-of-the-art semiconductor fabrication technology. Plasma based detonation of explosives using Semiconductor Bridge (SCB) has several significant advantages over conventional hot-bridgewire (HBW) based explosive initiation in electro explosive device due to its most excellent no-fire performance, low all-fire energy (requires small quantities of electrical energy to function), fast function time, light weight, small volume, low cost, need only small quantities of electrical energy and immunity to EMI (Electromagnetic interference), ESD (Electrostatic discharge) and RF (Radio Frequency) hazards. The study of surface nanomechanical properties of SCB is critical and essential, because the success of many applications is partly determined by a precise understanding of its mechanical characteristics. Therefore, determination of the mechanical properties of SCB becomes important. To probe the mechanical properties of the SCB, in the present work, ultra nano hardness testing (UNHT) is done by applying 10mN load. We have employed fatigue test to study the stability of the device where 25 cycles of varying load of 5mN – 2 mN is applied on Aluminium contact pads, poly silicon bridge and SiO_2 insulating layer. Results revealed that Aluminium contact pads shows fatigue behaviour after 15th cycle. Berkovich tip with a 70.3^{0} cone angle is used for the nanoindentation based fatigue test. Young's modulus and hardness were determined by the analysis of load-displacement curves using Oliver and Pharr method. X-ray Photoelectron Spectroscopy also was employed to determine elemental composition and chemical state information of the SCB surface.

The work had been presented at an international conference ***Fatigue Durability India 2015****, 28-30th May 2015, JN TATA AUDITORIUM, Indian Institute of Science, Bangalore.*
© 2015 JMSSE All rights reserved

Introduction

Electro-explosive devices (EEDs) are often used in military, industry and civil applications because of their characteristic features such as versatility and easy operation mode. Conversion of electrical energy into thermal energy is underlying principle of EEDs to start off an explosive chemical reaction. Now a day's demand for electro explosive devices is wide spread in the area of defence and civil application. To meet this demand researchers in defence area have successfully designed and developed different type of detonators.

Semiconductor bridge (SCB) igniters are advanced electro explosive devices [1] which are usually fabricated using state-of-the-art semiconductor fabrication technology. Plasma based detonation of explosives using Semiconductor Bridge (SCB) has several significant advantages over conventional hot-bridgewire (HBW) based explosive initiation in electro explosive device due to its most excellent no-fire performance, low all-fire energy (requires small quantities of electrical energy to function), fast function time, light weight, small volume, low cost, need only small quantities of electrical energy and immunity to EMI (Electromagnetic interference), ESD (Electrostatic discharge) and RF (Radio Frequency) hazards[2-7].

Armament Research and Development Establishment (ARDE) has successfully developed SCB igniter of various sizes and it has gone through series of rigorous military standard and qualification testing such as High & low temperature storage test, thermal shock test, Tropical Exposure Test, bump & jolt test, drop test, rain test, vibration test, salt spray test, acceleration test, etc.

Mechanical properties such as Elastic modulus, indentation hardness and stiffness are expected to influence the performance of SCB operation . Elastic modulus (E) reflects the resistance of a material to elastic deformation and is obtained from the slope of the linear region of a stress –strain relationship[8]. Hardness is a measure of the hardness or softness of a material and also represents the ability of a solid material to resist elastic deformation, plastic deformation and destruction [9].

Experimental

Nanoindentation

In a typical nanoindentation experiment, the indenter makes contact with the material surface and then penetrates to a depth. A typical nanoindentation curve is plotted for load (y-axis) as a function of displacement (x-axis) of the indenter and shows loading and unloading profile. Figure1 show a typical loading and

Corresponding author. Tel.: +91-9930465117
E-mail address: muthurajan@nano.mu.ac.in / muthurajan_h@yahoo.com
© 2015 JMSSE All rights reserved

unloading curve of nanoindentation on thin film materials. Any inconsistency observed in the curve indicates cracking, delamination or another failure such as fatigue in the coating or thin film. Also figure 1 shows the unloading process and parameters associated with the contact geometry.

The depth of penetration is considered to be displacement into the sample. The quantities which can be calculated from the stress-strain curve are the maximum depth of penetration (h_{max}), the peak load (P_{max}) and the final depth or displacement after unloading (h_r). The slope of the upper portion of the unloading curve is known as the contact stiffness (S). The hardness and modulus values are experimentally determined and discussed in the following section.

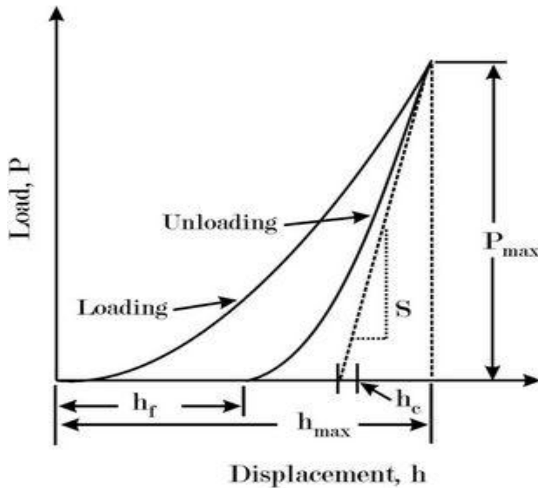

Figure 1: Typical load-displacement curve measured on nanoindenter tester.

Oliver and Pharr in 1992 proposed the method to determine the elastic moduli and hardness by nanoindentation which is being used most extensively for the characterization of mechanical behavior of materials at micro/nano scales [10]. The slope of the unloading curve which is usually nonlinear was used to calculate the elastic moduli of the material under testing.

Hardness and elastic modulus

The indentation hardness (equation 1) is calculated from the indentation load divided by the projected contact area.

$$H = \frac{P_{max}}{A} \qquad \ldots\ldots (1)$$

The indentation modulus is usually determined from the slope of the unloading curve at maximum load. Equation (2) shows that the indentation modulus (here expressed as E^*) as a function of dP/dh and the area of contact.

$$E^* = \frac{1}{2}\frac{\sqrt{\pi}}{\sqrt{A}}\frac{dP}{dh} \qquad \ldots\ldots (2)$$

The elastic modulus (E) of the test material is calculated from E_r using

$$\frac{1}{E_r} = \frac{1-\upsilon_f^2}{E_f} + \frac{1-\upsilon_i^2}{E_i} \qquad \ldots\ldots (3)$$

Where υ_f is the Poisson's ratio for the test material, and E_i and υ_i are the elastic modulus and Poisson's ratio of the indenter, respectively. For diamond, the elastic constants E_i = 1141 GPa and υ_i = 0.07 [11].

The basic parameters calculated from the applied force-displacement curves are the peak load (P_{max}), the displacement at peak load (h_t), the initial unloading contact stiffness (S). The calculation of contact depth (h_c) needs theoretical model assumptions following from the indenter geometry. The contact depth can be estimated using a formula as below :

$$h_c = h_t - \varepsilon\frac{P_{max}}{S} \qquad \ldots\ldots (4)$$

Where ε = 0.75 for a Berkovich indenter.

The projected contact area can be calculated by evaluation of an empirically determined indenter area function as below

$$A_c = 24.56\, h_c^2 \qquad \ldots\ldots (5)$$

Materials and Methods

A typical SCB device consists of H shaped thin poly silicon on SiO_2 layer on Silicon wafer or Silicon on Sapphire(SOS) film or Sapphire wafer and two metal lands are deposited over the outer legs of the H shaped film for electrical connection such that two metal lands forms a bridge . The length of the bridge (e.g. 100 μm) is determined by the spacing of the aluminium lands. Typically the doped polysilicon layer is 2 μm thick and the bridge is 380 μm wide. The 'H' shaped polysilicon layer is highly doped (~10^{20} cm^{-3}) with phosphorus impurities to achieve 1 Ω bridge resistance. The lands provide a low ohmic contact to the underlying doped layer. Wires ultrasonically bonded to the lands permit a current pulse to flow from land to land through the bridge. The current pulse through the SCB causes it to burst into a bright plasma discharge that heats the energetic powder pressed or slurry against it by a convective process that is both rapid and efficient. Consequently, SCB devices operate at very low energies and function very quickly. But despite the low energy for ignition, the substrate provides a reliable heat sink for excellent no-fire levels.

Results and Discussion

Hardness tests

During a nanoindentation test, a nanoindenter tip of known geometry is pressed into the surface with a predefined load or depth of penetration and the resultant affected area is recorded. The ratio of load over area determines the value of nanoindentation hardness.

To probe the mechanical properties of the SCB, in the present work Ultra Nano Hardness Testing (UNHT) is done. All nanoindentation tests were conducted in the continuous-stiffness-measurement (CSM) mode. The experimentally observed elastic modulus and hardness by us are summarized in table 1. The Poisson's ratio used [12 – 14] for the calculation of each layer (Aluminium, Polysilicon bridge, SiO_2) are also tabulated in table 1.

Table 1: Summary of nanoindentation results for the SCB

Material	Thickness (μm)	E (GPa)	H (MPa)	Poisson's ratio	Ref.
Aluminium	2	30.634	412.804	0.334	12
Bridge	2	109.602	9736.123	0.22	13
SiO_2	2	56.283	8028.805	0.17	14

As seen from figure 2, in the aluminium layer, the nanoindenter tip has created a permanent deformation depth around 850 nm (after unloading) of its actual thickness (2μm) for 10mN applied load showing plastic behaviour. Whereas polysilicon and SiO_2 shows elsto-plastic behaviour as they are showing less penetration depth as compare to Al-bridge interface and aluminium layer.

 © 2015 JMSSE All rights reserved

The load-displacement curve shows that aluminium is the softest material, with a peak depth of around 850 nm, while the hardest is polysilicon which was penetrated only about 50 nm. The other two layers shows varying degrees of elastic recovery during unloading.

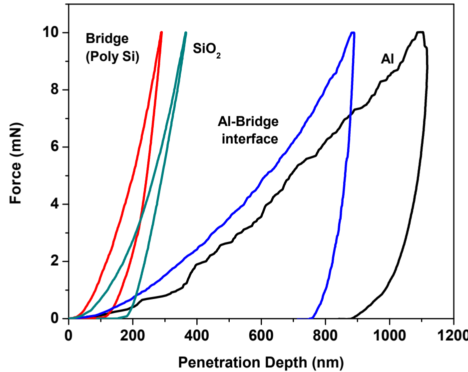

Figure 2 : Experimental load-displacement curves for the Aluminium, Polysilicon, Aluminum-Bridge interface and SiO_2 films.

Fatigue tests

We have employed fatigue test to study the stability of the device where 25 cycles of varying load of 5mN – 2 mN is applied on Aluminium contact pads, poly silicon bridge and SiO_2 insulating layer. The load was held constant for 10 seconds. Berkovich tip with a 70.3^0 cone angle is used for the nanoindentation based fatigue test.

Figure 3 shows the multicycle loading – unloading versus penetration depth for aluminium layer. Figure 4 shows the multicycle loading – unloading versus penetration depth on polysilicon (Bridge) layer. The multicycle loading – unloading versus penetration depth on SiO_2 layer is shown in figure 5.

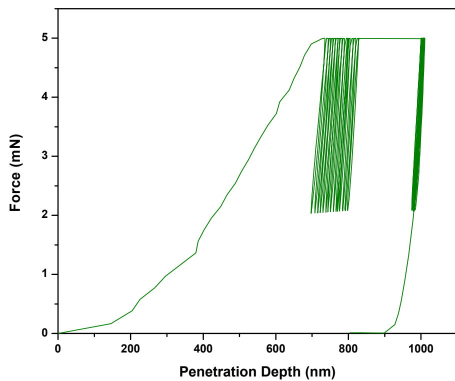

Figure 3 : Experimental curve of load versus penetration depth for aluminium.

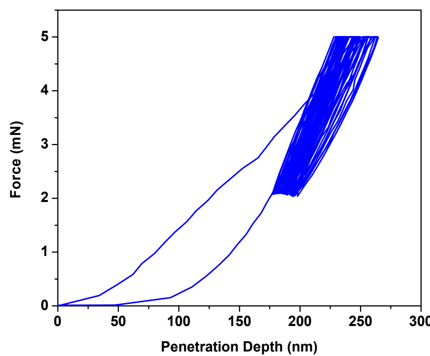

Figure 4 : Experimental curve of load versus penetration depth for Polysilicon (Bridge).

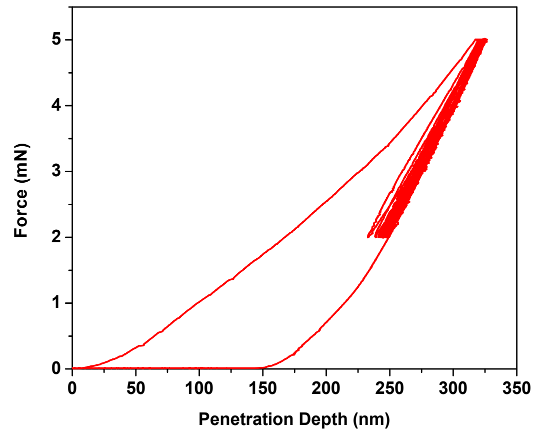

Figure 5 : Experimental curve of load versus penetration depth for SiO_2.

We have applied 25 cycles of 5mN of maximum load and 2mN of minimum load. It is revealed from the figures 3 to 5, that aluminum shows fatigue behavior after 15th cycle whereas no crack has been appeared on polysilicon and SiO_2 layer. In the case of aluminum for the constant applied load penetration depth goes on increasing and reaches upto about 850 nm at the 25th cycle. However for the same applied load and same number of cycles polysilicon and SiO_2 penetrates less indicating more elastic than aluminum. Creep has been observed in aluminum after 15th cycle of penetration of the indenter. Whereas polysilicon and SiO_2 does not show the creep in the whole 25 cycles of the penetration of the indenter.

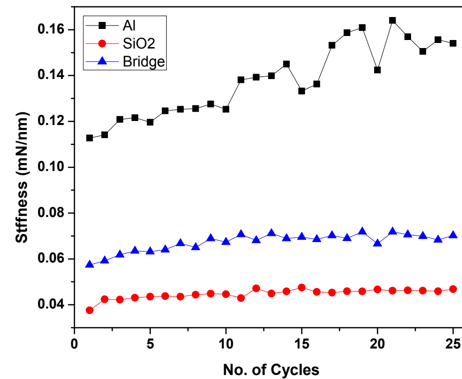

Figure 6 : Contact stiffness as a function of number of cycles for 2 micrometer thick aluminum, SiO_2 and Polysilicon layer.

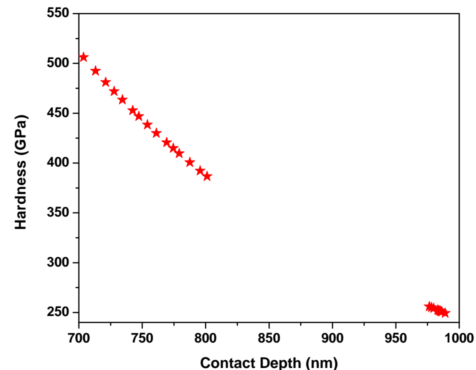

Figure 7: Hardness as a function of contact depth for aluminum.

© 2015 JMSSE All rights reserved

Figure 6 shows that there is increase in the stiffness of aluminum layer with respect to number of cycles while stiffness of polysilicon and SiO_2 remains constant as compared to aluminum with respect to number of cycles.

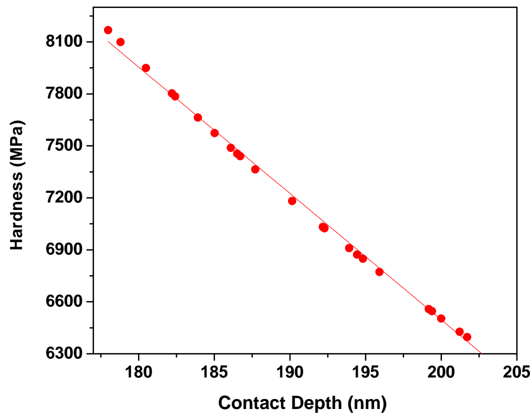

Figure 8: Hardness as a function of contact depth for Polysilicon.

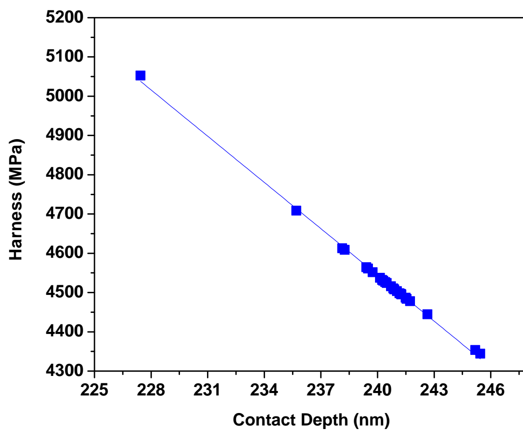

Figure 9: Hardness as a function of contact depth for SiO_2.

Decrease in hardness at the end of each cycle is observed on aluminum and shown in figure 7. On fitting the data points on linear fit for aluminum, we got the equation y= –0.837x + 1073 with correlation coefficient r^2=0.9908. A sudden discontinuity is observed in figure 7 is due to creep after 15th cycle.

Figure 8 shows that decrease in hardness of polysilicon at each cycle, on fitting the data points on linear fit, we got the equation y = –72.91 x + 21080 with correlation coefficient r^2=0.997. The hardness of SiO_2 is also decreases at the end of each cycle as shown in figure 9. On fitting the data points on linear fit for SiO_2 , we got the equation y= –0.39.25x + 13966 with correlation coefficient r^2=0.998.

Surface Analysis

X-ray Photoelectron Spectroscopy was employed to determine elemental composition of SCB surface and the spectra were obtained from a PHI 5000 Versa Probe. The SCB device were mounted on the sample holder using double-sided adhesive tape and placed into the vacuum chamber at a pressure of 1.3 X 10^{-7} torr. XPS was performed using the aluminium K-α x-ray source (1486.6eV) at 50 watts. The survey scan (pass energy of 117.40eV) has done at three different location of SCB chip in order to determine which elements were present on the surface of SCB Chip. A survey scan from 0 to 1400 eV was acquired for the sample and the elemental composition of the SCB's surface was determined using Multi Pack instrument software.

Elemental presences of Al and SiO_2 in the SCB sample were analyzed by X-ray photoelectron spectroscopy (XPS) results. Before the XPS measurement each layer was sputtered by Ar^{2+} for 2 min. in order to obtain a clear surface. The survey scan is shown in figure 10 and 11.

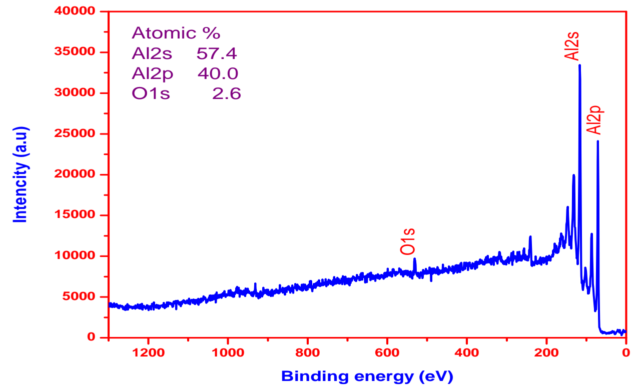

Figures 10 : The survey spectra of Al films of SCB.

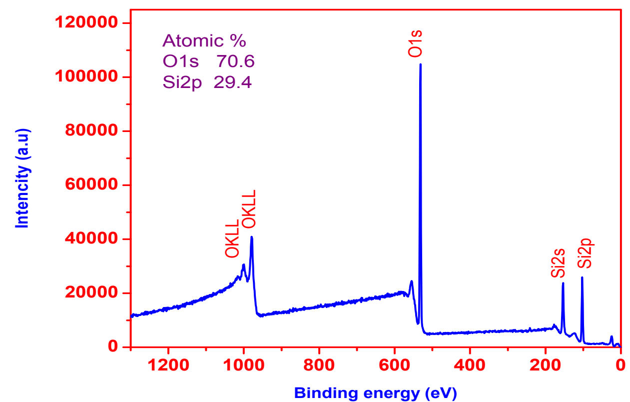

Figures 11 : The survey spectra of SiO_2 films of SCB.

The presence of an O1s peak at 532.4 eV in the Al spectra is due to the reoxidation of the substrate before XPS analysis (figure.10).The two prominent peaks at 154 eV (Si 2s) and 104.4 eV (Si 2 p) agreed well with the reported binding energies of SiO_2, which further confirmed the presence of SiO_2 film on the SCB surface (Figure 11).

Conclusions

We have applied 10mN force on aluminum, polysilicon (bridge) and SiO_2 layer of SCB and from the loading – unloading curve we observed that permanent deformation depth about 850 nm, 124nm, 175 nm respectively. When the samples are subjected to multiple cycles of loading – unloading, it is observed that the stiffness of Aluminum, polysilicon and SiO_2 layer increases. During multiple cycle of loading – unloading, it is observed that the hardness of aluminum, polysilicon and SiO_2 films decreases and a sudden rapid decrease in hardness is observed for aluminum after 15th cycle is due to creep. Using X-ray photoelectron spectrum, we have confirmed the presence of Aluminum, Silicon and Oxygen at the respective locations.

 © 2015 JMSSE All rights reserved

References

1. R. W. Bickes, (1988) Proceedings of 3rd Canadian Symp. on Mining Automation, Montreal, Quebec.
2. R. W. Bickes, Jr. S. E. Schlobohm, D. W. Ewick, (1988) Proceedings of Thirteenth International Pyrotechnic Seminar, Grand Junction Colorado, 69 – 80.
3. D.A. Benson, M.E. Larsen, A.M. Renlund, W.M. Trott, R.W. Bickes, (1987), J. Appl. Phys. 62 (5).
4. Jongdae Kim, EdlSchamiloglu, Bernardo Mertinez Tovar, Kenneth C. Jungling, (1995) IEEE Transactions on Instrumentation and Measurement, Vol 14, No. 4.
5. James L. Austing, Allen J. Tulis, Donald J. Hrdina, Richard P. Joyce, and Edward Urbanski, Donald W. Fyfe, Robert D. Smith, and Guy Letendre, (1988) Propellants, Explosives, Pyrotechnics 13, 129-13.
6. Ron Varosh, (1996) Propellants, Explosives, Pyrotechnics 21, 150-154.
7. B. A. M. Tovar, (1993) Univ. of New Mexico Press, New Mexico.
8. Shu DL, Chen JB, Feng Y. (2006), Engineering material mechanics, Beijing: China Machine Press; 2–5.
9. Chen ZQ, Zhang M, Zhang JK.(2008), Oral materials. 4th ed. Beijing: People's Medical Publishing House, 18–19.
10. W.C. Oliver and G.M. Pharr, (1992) , J. Mater. Res., 1564.
11. G. Simmons and H. Wangs (1971), A Handbook 2nd ed, The M.I.T. Press, Cambridge, Massachusetts.
12. James M. Gere, Stephen P. Timoshenko, (1997), Mechanics of Material, 4th edition, PWS Pub Co.
13. W.N.Sharpe, Jr., Bin Yuan, R.L.Edwards, and R. Vaidyanathan, (1997),10th IEEE International Workshop on Microelectromechanical Systems, Nagoya, Japan.
14. J. Eo Greene (1996), Thin Solid Films, Volume 283,p.15.

 © 2015 JMSSE All rights reserved